# Phase transitions and modulated phases in lipid bilayers

C.-M. Chen,[1] T.C. Lubensky,[2] and F.C. MacKintosh[1]
[1]*Department of Physics, University of Michigan, Ann Arbor, Michigan 48109-1120*
[2]*Department of Physics, University of Pennsylvania, Philadelphia, Pennsylvania 19104*
(Received 20 June 1994)

We develop and analyze a continuum Landau theory for ordered chiral and achiral bilayer membranes. This theory contains couplings between tangent-plane orientational order and curvature that lead to "rippled" or $P_{\beta'}$ phases with one-dimensional height modulations and to phases with two-dimensional height modulations. We calculate mean-field phase diagrams from this model.

PACS number(s): 61.30.Cz, 64.60.−i, 64.70.Md

## I. INTRODUCTION

Lipid molecules have charged or polar heads and one or two hydrocarbon tails. When dissolved in water at sufficient concentration, they self-assemble into bilayer membranes in which their oily tails are shielded from contact with the surrounding water. Under appropriate conditions, lamellar phases consisting of periodically spaced parallel membranes separated by water are the equilibrium phases. Membranes in lamellar phases as well as isolated membranes (e.g., in closed vesicles) can exhibit varying degrees of order. It is customary to classify membrane order according to the equilibrium lamellar phase whose membranes exhibit that order. There is the $L_\alpha$ or fluid phase [1] in which the long axes of constituent molecules, like those of a smectic-$A$ liquid crystal, are on average parallel to the membrane or layer normal. There are the $L_{\beta'}$ phases [1] in which long molecular axes, like those in a smectic-$C$ liquid crystal, tilt on average relative to the membrane or layer normal. The molecular tilt defines a two-dimensional tangent-plane order parameter. The $L_{\beta'}$ phases, of which there are three, also exhibit hexatic bond-angle order and are distinguished from each other by the angle the tilt direction makes with the direction of hexatic order [2]. Finally, there is the rippled or $P_{\beta'}$ phase [1,2]. This phase, whose lamellar realization is depicted schematically in Fig. 1, is characterized by a one-dimensional height modulation of each membrane [1–6] in addition to nonzero tilt [1,3]. The height modulations of the lamellar $P_{\beta'}$ phase have two-dimensional crystalline symmetry in the plane containing the layer normals and the membrane modulation vector. In the direction perpendicular to this plane, there is only fluidlike short-range order if the membranes themselves have only orientational order, not crystalline order. A schematic representation of the phase diagram for dimyristoyl phosphatidylcholine (DMPC) in the temperature–relative-humidity plane is shown in Fig. 2.

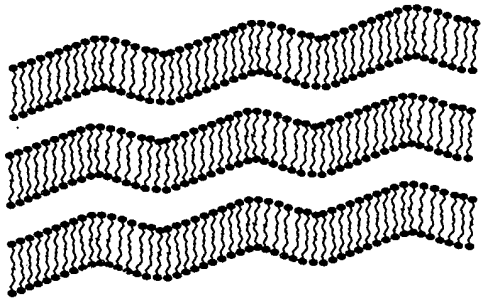

FIG. 1. Schematic representation of rippled membranes in the $P_{\beta'}$ phase. The ripples are asymmetric, and there is a phase shift in the ripple pattern from layer to layer producing a two-dimensional oblique lattice.

In this paper, we present and analyze a phenomenological Landau model [7] for tilted bilayer membranes that includes coupling between tangent-plane order and membrane shape (or curvature) and chiral couplings present when constituent molecules are chiral. This model predicts phase transitions from the $L_\alpha$ phase to the tilted $L_{\beta'}$ phases. It also predicts the possible existence of a number of distinct rippled phases distinguished by height

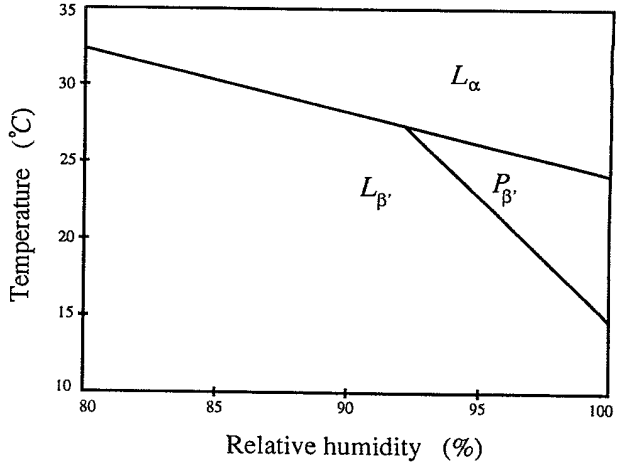


FIG. 2. The phase diagram of DMPC-water as a function of temperature and relative humidity, showing the $L_\alpha$, $L_{\beta'}$, and $P_{\beta'}$ phases. The $P_{\beta'}$ phase occurs for relative humidity greater than 90% and for temperatures between 15 and 30 °C. This range corresponds to water content greater than approximately 20%. Additional tilted hexatic phases ($L_{\beta F}$, $L_{\beta L}$, $L_{\beta I}$) are not shown in this figure [2].

 

profiles of different symmetry and by different tilt-order-parameter configurations relative to the ripples. Ripple configurations with five distinct symmetries, as shown in Fig. 3, are possible. Our model predicts the shape (a) in Fig. 3 for achiral systems and shapes (a), (b), and (c) in Fig. 3 for chiral systems. The asymmetric shape shown in Fig. 3(b) most closely resembles that observed experimentally, though symmetric shapes such as that in Fig. 3(a) have also been reported. Finally, the model predicts the possible existence of phases with two-dimensional rather than one-dimensional height modulations.

Before describing the present work in detail, we find it useful to review the experimental evidence for the $P_{\beta'}$ phase and previous theoretical models for this phase. The $P_{\beta'}$ phase was first observed by Tardieu *et al.* [1] in x-ray scattering experiments on lamellar phases of lecithins. It exists in regions of high water content. Its ripple structure is a corrugation such as that shown in Fig. 1 rather than a peristaltic modulation of membrane thickness. The evidence for this comes from the large amplitude (45 Å) of the ripples compared to the membrane thickness (60 Å) observed in freeze-fracture scanning tunneling microscope (STM) measurements and from x-ray scattering [5,8]. The ripple wavelength is a function of both temperature and water content [3,6] and varies between 140 Å and 200 Å. Both symmetric and asymmetric ripples such as those depicted schematically in Figs. 3(a) and 3(b) have been inferred from x-ray diffraction patterns [1,4,6,9] and from freeze-fracture experiments [10]. In particular, two-dimensional x-ray diffraction patterns with Bragg peaks on an oblique rather than a rectangular lattice indicate an asymmetric ripple pattern with a phase shift between layers as shown in Fig. 1. Only the shape shown in Fig. 3(b) can produce such a diffraction pattern. In keeping with common usage in the literature, we shall refer to this shape as the asymmetric ripple although several ripple structures with lower symmetry than the symmetric structure shown in Fig. 3(a) are possible. The degree of symmetry can depend on water content. Reference [6] reports that the reciprocal lattice of Bragg peaks approaches rectangular symmetry as water content is increased.

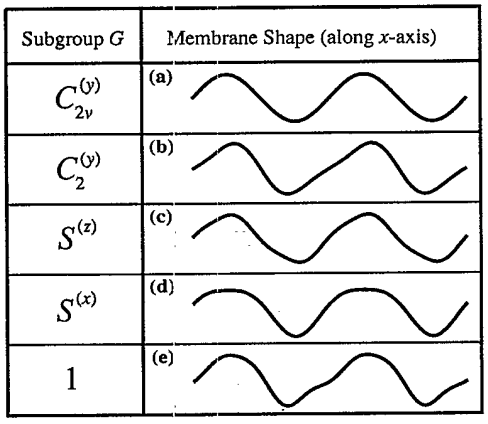


FIG. 3. Ripple symmetries ($G \times S_y^{(y)}$) with corresponding membrane shapes undulating in the $x$ direction.

Our model for chiral lipids such as DMPC yields asymmetric ripples consistent with observed structures. In contrast with the bend stripe patterns in chiral smectic-$C^*$ (Sm-$C^*$) films [11], the ripple structure of the $P_{\beta'}$ phase is not directly caused by the molecular chirality. In Ref. [12] mixtures of enantiomers of dipalmitoyl phosphatidylcholine (DPPC) with opposite chirality were studied in excess water. A ripple phase was observed for all mixtures, including the achiral racemic mixture. Furthermore, the relative concentration of right- and left-handed molecules had no significant effect on the ripple wavelengths or the transition temperatures. Although Ref. [12] reported asymmetric ripples in the pure systems, it did not undertake a systematic study of ripple symmetry. In our model, the degree of ripple asymmetry is predicted to depend on the chirality. In particular, symmetric ripples are predicted for an achiral system.

Less is known about the molecular tilt than about the shapes of the membranes in the ripple phase. While the existence of molecular tilt in the ripple phase has been established, in most cases only an average tilt angle has been inferred from the layer spacing and bilayer thickness. It is apparent, however, that the molecular orientation is not constant in space [13], as has been suggested by several previous theoretical models. Furthermore, recent experiments suggest that the $P_{\beta'}$ phase is characterized by nonzero molecular tilt transverse to the ripple wave vector [9], as predicted by our model.

We now describe briefly previous theoretical models of the $P_{\beta'}$ phase. The models of Falkovitz *et al.* [14], and later of Marder *et al.* [15] describe the bilayer ripple as a modulation in layer thickness. Goldstein and Leibler [16] proposed a similar model, to which they added interlayer interactions due to van der Waals and hydration forces. However, the order parameter in these theories is a scalar: the layer thickness. As noted in Ref. [16], such a description does not account for the different symmetries of the $L_\alpha$, $L_{\beta'}$, and $P_{\beta'}$ phases. The authors of Ref. [16] were concerned primarily with the role of interlayer interactions. Furthermore, these models do not provide a mechanism for the instability of flat membranes. X-ray diffraction data as well as the observed ripple amplitude are inconsistent with a modulation in layer thickness, as proposed by these theories. Interactions between layers, as introduced in Ref. [16] may also play an important role. However, ripple structures in isolated membranes have recently been observed [10] indicating that intermembrane interactions are not essential for the production of ripples. In contrast, the models of Doniach [17] and of Carlson and Sethna [18] are based on the microscopic packing properties of the lipid molecules. These models describe the ripple phase as one in which the membranes (of nearly constant thickness) undulate, while the orientation of the molecules is constant in space. Although this picture is in better qualitative agreement with known structural properties of the ripple phase, these *one-dimensional* models only account for molecular tilt in the direction of the ripple (i.e., *longitudinal* tilt). Thus, they describe only the symmetric $P_{\beta'}^{(2)}$ phase of our theory. We expect on quite general grounds

that the transition from the flat tilted phase ($L_{\beta'}$) to the rippled phase will involve a modulation of the membrane perpendicular to the direction of the tilt. In essence, a modulation transverse to the tilt direction corresponds to a soft mode of the $L_{\beta'}$ phase, while a longitudinal modulation is disfavored.

In a previous paper [7], we introduced a phenomenological model of $P_{\beta'}$ phases that can account for the observed ripple phases. We showed that, while the apparent ripple structure is essentially one dimensional, the two-dimensional nature of the molecular tilt in the membranes can lead to an unexpected variety of modulated phases of different symmetry. In this paper, we first classify the various possible ripple symmetries that can occur. We then describe our model for both achiral and chiral membranes, with particular emphasis on the $P_{\beta'}$ phases. Another modulated structure that has been widely studied is that of the chiral stripe phases of, for example, Sm-$C^*$ films [11]. Thus we include a discussion of the effects of the coupling of molecular tilt to membrane curvature in these phases. In particular, we show that these stripe phases are always rippled unless they are constrained to lie flat or are infinitely rigid. We also show that they can undergo a curvature-induced period-doubling transition.

## II. RIPPLE SHAPES AND SYMMETRIES

We begin with a discussion of the possible one-dimensional ripple symmetries without regard for the molecular tilt within the membrane. For a nearly flat membrane, the shape can be described by a function $h(x,y)$, the height of the membrane above a reference $x$-$y$ plane. For one-dimensional ripples, such as are observed in the $P_{\beta'}$ phase, the membrane shape can be completely characterized by a function of a single variable, $h(x)$. A flat membrane is symmetric under arbitrary translations and rotations of the $x$-$y$ plane, as well as the discrete symmetry group $D_{2h}$, the group of order-2 rotations about the three coordinate axes together with space inversion [19,20]. The full point-group symmetry of the flat membrane is actually $D_{\infty h}$, since arbitrary rotations preserve the membrane shape. Any purely one-dimensional ripple structure is symmetric under $\sigma_y$ (the reflection $y \to -y$). Thus, apart from discrete translations of the membrane, the possible symmetry groups are of the form $G \times S^{(y)}$, where $S^{(y)} = \{1, \sigma_y\}$. There are five possibilities for the subgroup $G$: $C_{2v}^{(y)}, C_2^{(y)}, S^{(x)}, S^{(x)}, \{1\}$. The corresponding membrane shapes are shown in Fig. 3. Of these possible shapes, at least the first two seem to have been observed. The second shape is what has been referred to as an asymmetric ripple in the literature. In addition to the first shape, for chiral lipids, our model predicts the second and third shapes for certain phases. Experimental reports of x-ray diffraction, however, do not distinguish between shapes (a) and (c).

Although the observed ripple structures of the $P_{\beta'}$ phase are essentially one dimensional, the existence of orientational order (in the form of molecular tilt) within the membrane can lead to additional phases of different symmetry. In particular, the full symmetry group $D_{2h}$ for one-dimensional modulations of both membrane shape and molecular orientation must be considered. A complete description of all possible symmetries will not be given here. However, we note that $D_{2h}$ has 16 possible subgroups. Below, we indicate the symmetry groups for the various ripple phases predicted by our model.

## III. THE MODEL FOR ACHIRAL BILAYERS

In this section, we develop a phenomenological Landau theory for tilt order and curvature of a single membrane [21]. As shown in Fig. 4, the molecular orientation determines a vector order parameter, $\mathbf{m}$, defined in the plane tangent to the surface. We include the coupling of molecular tilt to membrane curvature that is ultimately responsible for the production of ripples in this model. This coupling results from steric interactions between neighboring molecules, as illustrated in Fig. 5. A divergence of $\mathbf{m}$ corresponds to a varying tilt angle of the molecules relative to the surface, which gives rise to a *spontaneous curvature* of the membrane. This coupling of the tilt to curvature reduces the in-plane tilt elastic constant. Our model [7] is similar to the Landau theory of the smectic-$A$–to–smectic-$C$ transition in liquid crystals. The model free energy involves only quadratic and quartic terms that are allowed by rotational symmetry in the tangent plane:

$$f_m = \frac{1}{2}C_{\parallel}(\nabla \cdot \mathbf{m})^2 + \frac{1}{2}C_{\perp}(\nabla \times \mathbf{m})^2 + \frac{1}{2}D\left(\nabla^2 \mathbf{m}\right)^2 + \frac{1}{2}t|\mathbf{m}|^2 + u|\mathbf{m}|^4. \quad (1)$$

This is a Lifshitz [22] free energy that produces equilibrium modulated phases if either $C_{\parallel}$ or $C_{\perp}$ is negative [in which case the $\left(\nabla^2 \mathbf{m}\right)^2$ term is needed for stability]. Because of the vector nature of the order parameter, no cubic term is allowed. The first terms represent the tilt elasticity in the tilted phase. These correspond to splay and bend, respectively. To these elastic terms we add the curvature energy

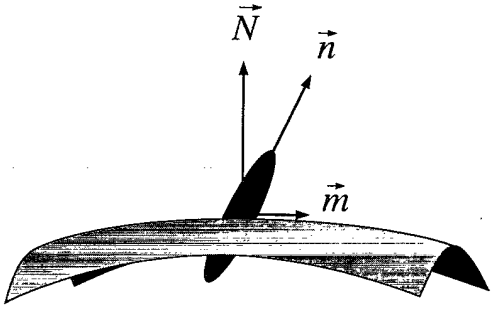


FIG. 4. Smectic-$C$ order within a fluid membrane arises from a tilt of the constituent molecules (represented by the solid oval and unit director $\mathbf{n}$) relative to the unit membrane normal $\mathbf{N}$. The surface component, $\mathbf{m} = \mathbf{n} - (\mathbf{N} \cdot \mathbf{n})\mathbf{N}$, represents a two-dimensional vector order parameter.

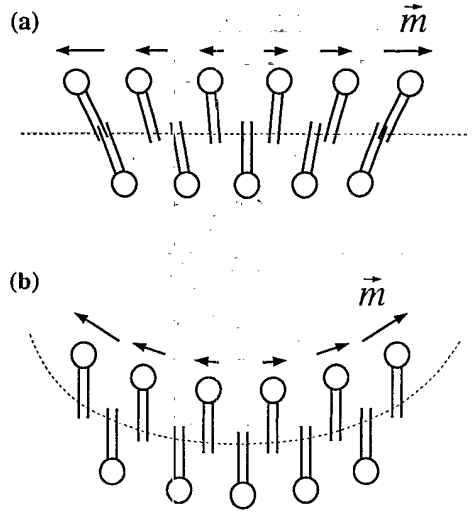


FIG. 5. An illustration of the microscopic origin of the coupling between tilt and curvature within a membrane. A divergence of the tilt $\mathbf{m}$ gives rise to a spontaneous curvature of the membrane (b).

$$f_c = \frac{1}{2}\kappa\left(\nabla^2 h\right)^2 - \gamma\left(\nabla^2 h\right)(\boldsymbol{\nabla}\cdot\mathbf{m}), \tag{2}$$

including the allowed coupling of gradients in tilt to the mean membrane curvature [23]. Here, $h(x,y)$ is the height of the membrane relative to some flat plane with coordinates $(x,y)$, and $\nabla_i\nabla_j h(x,y)$ is the curvature tensor. (Covariant forms of the terms in Eqs. (1) and (2) were shown in another context in Ref. [24].)

The equilibrium membrane shape can be determined by minimization of the free energy in Eqs. (1) and (2). This shape is determined by

$$\boldsymbol{\nabla}^2 h = \frac{\gamma}{\kappa}(\boldsymbol{\nabla}\cdot\mathbf{m}). \tag{3}$$

When $h$ is replaced by this equilibrium value in the presence of a nonvanishing $\boldsymbol{\nabla}\cdot\mathbf{m}$, the result is an effective free energy identical to Eq. (1) but with a reduced longitudinal elastic constant

$$C_{\parallel}' = C_{\parallel} - \gamma^2/\kappa. \tag{4}$$

Thus the effective free energy is given by

$$f_{\text{eff}} = \frac{1}{2}C_{\parallel}'(\nabla\cdot\mathbf{m})^2 + \frac{1}{2}C_{\perp}(\nabla\times\mathbf{m})^2 + \frac{1}{2}D\left(\nabla^2\mathbf{m}\right)^2 + \frac{1}{2}t|\mathbf{m}|^2 + u|\mathbf{m}|^4. \tag{5}$$

When $C_{\parallel}' > 0$, the equilibrium phases are spatially uniform; when $C_{\parallel}' < 0$, modulated phases are possible with a characteristic wave vector $q_0 = (2\pi/\lambda) = \sqrt{|C_{\parallel}'|/2D}$ that tends to zero at $C_{\parallel}' = 0$. Thus, as the membrane rigidity is reduced (say, by increasing hydration), the $L_{\beta'}$ phase becomes unstable to a ripple phase ($P_{\beta'}$) with decreasing wavelength.

To determine the mean-field phase diagram, we restrict our attention to the single-mode approximation, in which the modulated phases are characterized by a single wave vector $q$. This should be valid near the transition to the $L_\alpha$ phase. In this limit, all possible stable and metastable ripple phases can be expressed by the variational order parameter

$$m_x = m_1^L\cos(qx), \tag{6a}$$
$$m_y = m_0 + m_1^T\sin(qx). \tag{6b}$$

It can be shown, for instance, that no stable phase is possible with a constant longitudinal component, in contrast with the one-dimensional models of Refs. [17] and [18]. For simplicity, we have assumed that the one-dimensional modulated phases are rippled only in the $x$ direction. Three distinct phases are possible. These are shown in Figs. 6 and 7. In addition, we find a possible two-dimensional modulated phase shown in Fig. 7. Within the single-mode approximation, the tilt field in this phase can be expressed as

$$m_x = m_1\cos(qx), \tag{7a}$$
$$m_y = m_1\cos(qy). \tag{7b}$$

We shall call these phases $P_{\beta'}^{(1)}$, $P_{\beta'}^{(2)}$, $P_{\beta'}^{(3)}$, and the square lattice vortex phase. The first three phases are characterized by symmetric ripples: i.e., ignoring molecular tilt, they are symmetric under reflection through the midplane followed by a translation. The symmetric $P_{\beta'}^{(1)}$ and $P_{\beta'}^{(2)}$ phases both have a sinusoidally varying longitudinal component of the tilt field, $m_x$; they differ, however, in that the transverse component of the tilt field, $m_y$, is zero in the $P_{\beta'}^{(2)}$ phase but nonzero in the $P_{\beta'}^{(1)}$ phase. The achiral $P_{\beta'}^{(3)}$ phase is a spiral phase in which $\mathbf{m}$ makes one

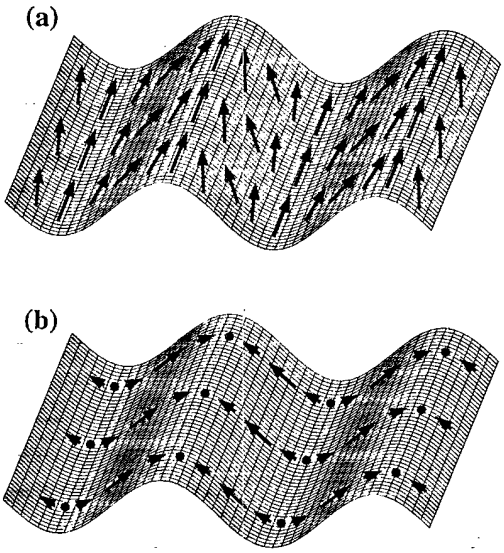


FIG. 6. A representation of the vector order parameter $\mathbf{m}$ with corresponding membrane shape in the symmetric $P_{\beta'}^{(1)}$ (a) and $P_{\beta'}^{(2)}$ (b) phases.

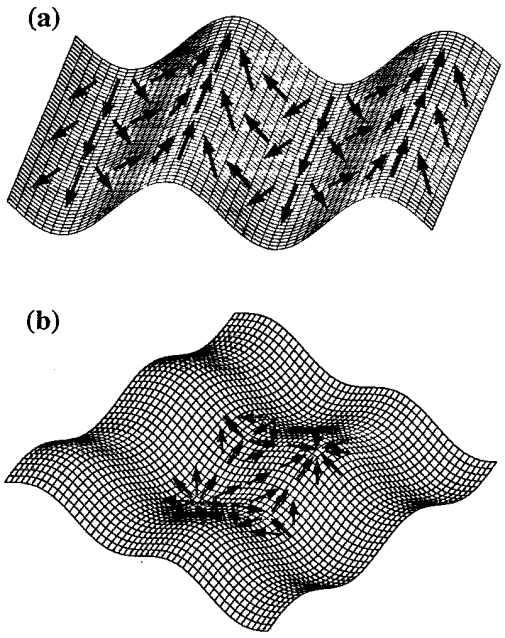


FIG. 7. A representation of the vector order parameter $\mathbf{m}$ with corresponding membrane shape in the symmetric $P_{\beta'}^{(3)}$ phase (**a**) and the square lattice phase (**b**).

complete revolution in a spatial period. More precisely, in the $P_{\beta'}^{(1)}$ phase $m_0 \neq 0$ and $m_1^L \neq m_1^T = 0$; in the $P_{\beta'}^{(2)}$ phase $m_0 = m_1^T = 0$ and $m_1^L \neq 0$; in the $P_{\beta'}^{(3)}$ phase $m_0 = 0$, $m_1^L = m_1^T \neq 0$. Thus the $P_{\beta'}^{(3)}$ phase has winding number 1, while the $P_{\beta'}^{(1)}$ and $P_{\beta'}^{(2)}$ phases have winding number 0. The square lattice phase exhibits a two-dimensional modulated structure. As depicted in Fig. 8, the tilt order parameter exhibits a vortex-antivortex square lattice, with two strength +1 vortices located at two corners and two strength −1 vortices located at the other corners.

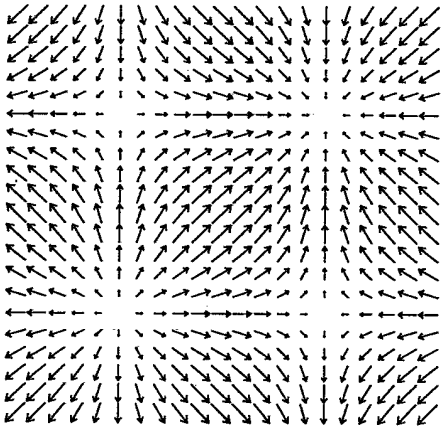

FIG. 8. A representation of the vector order parameter $\mathbf{m}$ of the square lattice phase within one unit cell.

Within the mean-field approximation, we calculate the free energy of $P_{\beta'}^{(1)}$, $P_{\beta'}^{(2)}$, $P_{\beta'}^{(3)}$, and the square lattice phase, denoted by $f_1$, $f_2$, $f_3$, and $f_4$, respectively. Here, we consider the average density of the free energy in Eq. (5) over one spatial period:

$$\langle f_{\rm eff}\rangle \equiv \frac{\iint f_{\rm eff}\, dx\, dy}{\iint dx\, dy}. \tag{8}$$

For $\mathbf{m}$ given by Eqs. (6a) and (6b), the free energy can be expressed as

$$\langle f_{\rm eff}\rangle = \frac{1}{4}C_{\parallel}' q^2 \left(m_1^L\right)^2 + \frac{1}{4}C_{\perp} q^2 (m_1^T)^2 + \frac{1}{4}Dq^4[\left(m_1^L\right)^2 + (m_1^T)^2] + \frac{1}{2}t\left[m_0^2 + \frac{1}{2}\left(m_1^L\right)^2 + \frac{1}{2}(m_1^T)^2\right]$$
$$+u\left(m_0^4 + m_0^2\left[\left(m_1^L\right)^2 + 3\left(m_1^T\right)^2\right] + \frac{1}{8}\left[3\left(m_1^L\right)^4 + 3\left(m_1^T\right)^4 + 2\left(m_1^L m_1^T\right)^2\right]\right). \tag{9}$$

In the $P_{\beta'}^{(1)}$ phase, the free energy minimum occurs for

$$q^2 = -\frac{C_{\parallel}'}{2D}, \tag{10}$$

$$\left(m_1^L\right)^2 = \frac{C_{\parallel}'^2}{4uD}, \tag{11}$$

and

$$m_0^2 = -\frac{1}{4u}\left(t + \frac{C_{\parallel}'^2}{2D}\right), \tag{12}$$

provided that $C_{\parallel}' < 0$ and $t < -C_{\parallel}'^2/2D$. In this case, the free energy of the $P_{\beta'}^{(1)}$ phase is given by

$$f_1 = -\frac{1}{16u}\left(t^2 + \frac{C_{\parallel}'^4}{8D^2}\right). \tag{13}$$

In the $P_{\beta'}^{(2)}$ phase, the free energy minimum occurs for

$$q^2 = -\frac{C_{\parallel}'}{2D} \tag{14}$$

and

$$\left(m_1^L\right)^2 = -\frac{1}{3u}\left(t - \frac{C_{\parallel}'^2}{4D}\right), \tag{15}$$

provided that $C_{\parallel}' < 0$ and $t < C_{\parallel}'^2/4D$. In this case, the

free energy of the $P_{\beta'}^{(2)}$ phase is given by

$$f_2 = -\frac{1}{24u}\left(t - \frac{C_{\parallel}'^2}{4D}\right)^2. \quad (16)$$

In the $P_{\beta'}^{(3)}$ phase, the free energy minimum occurs for

$$q^2 = -\frac{\left(C_{\parallel}' + C_{\perp}\right)}{4D} \quad (17)$$

and

$$\left(m_1^L\right)^2 = -\frac{1}{4u}\left(t - \frac{\left(C_{\parallel}' + C_{\perp}\right)^2}{16D}\right), \quad (18)$$

provided that $C_{\parallel}' < -C_{\perp}$ and $t < \left(C_{\parallel}' + C_{\perp}\right)^2/16D$. In this case, the free energy of the $P_{\beta'}^{(3)}$ phase is given by

$$f_3 = -\frac{1}{16u}\left(t - \frac{\left(C_{\parallel}' + C_{\perp}\right)^2}{16D}\right)^2. \quad (19)$$

In the square lattice phase, the free energy can be expressed as

$$\langle f_{\text{eff}}\rangle = \frac{1}{2}C_{\parallel}'q^2m_1^2 + \frac{1}{2}Dq^4m_1^2 + \frac{1}{2}tm_1^2 + \frac{5}{4}um_1^4. \quad (20)$$

The free energy minimum occurs for

$$q^2 = -\frac{C_{\parallel}'}{2D} \quad (21)$$

and

$$m_1^2 = -\frac{1}{5u}\left(t - \frac{C_{\parallel}'^2}{4D}\right), \quad (22)$$

provided that $C_{\parallel}' < 0$ and $t < C_{\parallel}'^2/4D$. In this case, the free energy of the square lattice phase is given by

$$f_4 = -\frac{1}{20u}\left(t - \frac{C_{\parallel}'^2}{4D}\right)^2. \quad (23)$$

To study the stability of these phases, we compare $f_1$, $f_2$, $f_3$, and $f_4$ with each other. By comparing $f_4$ with $f_2$, we find that the free energy of $P_{\beta'}^{(2)}$ is always higher than that of the square lattice phase. So $P_{\beta'}^{(2)}$ is never the equilibrium for the model in Eqs. (1) and (2). (Since our model ignores free energy contributions due to the Gaussian curvature of the membrane, which are higher order than the terms included above, the $P_{\beta'}^{(2)}$ phase is expected to be stabilized relative to the square lattice phase away from the Lifshitz point. Thus, for instance, in the presence of positional order or hexatic order within the membrane, the $P_{\beta'}^{(2)}$ phase may occur.) By solving $f_4 = f_1$, we find that the first-order transition between $P_{\beta'}^{(1)}$ and the square lattice phase occurs at $t_{c1} \cong -1.79C_{\parallel}'^2/D$. The stability of the square lattice phase is also determined by comparing $f_4$ and $f_3$. The first-order transition between $P_{\beta'}^{(3)}$ and the square lattice phase occurs at $t_{c2} \cong -1.53C_{\parallel}'^2/D + 1.18C_{\parallel}'C_{\perp}/D + 0.59C_{\perp}^2/D$. However, the square lattice phase is unstable to the uniform $L_\alpha$ above $t_{c3} = C_{\parallel}'^2/4D$. Finally, the phase boundary between $P_{\beta'}^{(1)}$ and $P_{\beta'}^{(3)}$ has also been determined by solving $f_1 = f_3$. The phase diagram for this model is shown in Fig. 9.

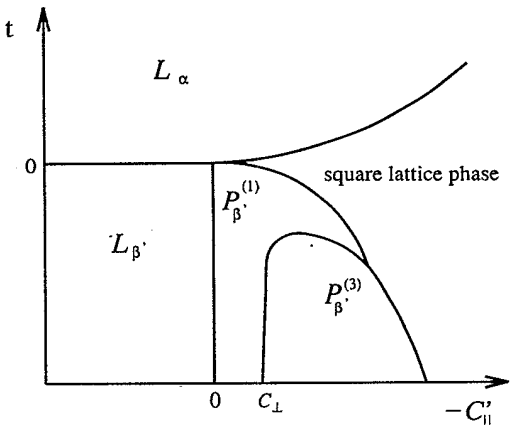


FIG. 9. The mean-field phase diagram of achiral membranes by varying $C_{\parallel}'$ and t. The modulated $P_{\beta'}^{(1)}$ and square lattice phases meet the $L_\alpha$ and $L_{\beta'}$ phases at the Lifshitz point where order first develops. As the temperature is lowered, there is a first-order transition from the $P_{\beta'}^{(1)}$ phase to the spiral $P_{\beta'}^{(3)}$ phase.

## IV. THE MODEL FOR CHIRAL MEMBRANES

For chiral membranes, additional chiral terms must be included in Eqs. (1) and (2) because of the absence of inversion symmetry. These terms may be due to the chiral nature of the lipid constituents. However, the packing of lipid molecules in a membrane can result in spontaneously broken chiral symmetry, even for achiral molecules or for a racemic mixture [25]. The lowest-order chiral coupling allowed in Eq. (1) for bilayer membranes is $\lambda_b|\mathbf{m}|^2(\nabla \times \mathbf{m})$ [26–29]. To Eq. (2) we must add the chiral coupling of tilt to membrane shape. As described by Helfrich and Prost [30], the tendency of chiral molecules to twist in three dimensions leads to the following free energy contribution for two-dimensional membranes that are allowed to curve in three dimensions:

$$f_{\text{HP}} = \lambda_{\text{HP}}\epsilon_{ki}(\nabla_i\nabla_j h)m_j m_k. \quad (24)$$

As in the previous section, the effective free energy in terms of the tilt $\mathbf{m}$ can be found by a functional min-

imization of the free energy with respect to the shape profile $h(x,y)$. The result is

$$f_m = \frac{1}{2}C_{\parallel}'(\nabla\cdot\mathbf{m})^2 + \frac{1}{2}C_{\perp}(\nabla\times\mathbf{m})^2 + \frac{1}{2}D(\nabla^2\mathbf{m})^2 + \frac{1}{2}t|\mathbf{m}|^2 + u|\mathbf{m}|^4 + \lambda_b'|\mathbf{m}|^2(\nabla\times\mathbf{m}), \quad (25)$$

where $C_{\parallel}'$ is given by Eq. (4) and

$$\lambda_b' = \lambda_b + \frac{\lambda_{\rm HP}\gamma}{2\kappa}. \quad (26)$$

Furthermore, the equilibrium membrane shape $h(x,y)$ satisfies

$$\nabla^4 h = \frac{\gamma}{\kappa}\nabla^2(\nabla\cdot\mathbf{m}) - \frac{\lambda_{\rm HP}}{\kappa}\epsilon_{ki}[\nabla_i\nabla_j(m_j m_k)]. \quad (27)$$

The shapes of the various one-dimensional ripple phases (with assumed variation in the $x$ direction) can be determined from the solutions of Eq. (25) together with

$$\frac{d^2h}{dx^2} = \frac{\gamma}{\kappa}\frac{dm_x}{dx} + \frac{\lambda_{\rm HP}}{\kappa}m_x m_y. \quad (28)$$

Each of the resulting profiles can be expressed in a Fourier series:

$$h(x) = a_1\sin(qx) + a_2\sin(2qx) + b_2\cos(2qx) + a_3\sin(3qx) + b_3\cos(3qx) + \cdots. \quad (29)$$

For example, we find that $a_2 \neq 0$ in the $P_{\beta'}^{(3*)}$ phase, as shown in Fig. 3(b). Thus the chiral terms above convert the $P_{\beta'}^{(3)}$ phase into an asymmetric $P_{\beta'}^{(3*)}$ phase, the shape of which is consistent with the asymmetric ripples observed in numerous experiments. The $P_{\beta'}^{(2)}$ phase is not affected by the addition of chiral terms. The symmetry of the chiral $P_{\beta'}^{(1*)}$ phase is lower than that of the $P_{\beta'}^{(1)}$ phase with $b_3 \neq 0$ and $a_2 = 0$. Its shape is that of (c) in Fig. 3.

Additional chiral phases, such as the chiral stripe phase and hexagonal phase of Refs. [27–29], can occur for large $\lambda_b$ in the region of positive $C_{\parallel}'$. The appearance of these modulated phases is due to the fact that the chiral term will effectively reduce the bend elastic constant $C_{\perp}$, leading to an instability of the flat membrane. For $\lambda_b > \sqrt{2uC_{\perp}}$, the equilibrium phase is the bend stripe phase of Ref. [27]. Although it is characterized primarily by bend, this phase also exhibits a splay modulation—i.e., $\nabla\cdot\mathbf{m} \neq 0$. As a result of the coupling between splay and curvature in Eq. (2) and Fig. 5, this phase also exhibits a ripple structure. The shape of this $P_{\beta'}^{(4*)}$ phase can be obtained from Eq. (3). It is interesting to note that the $P_{\beta'}^{(3*)}$ phase and the chiral stripe phase, $P_{\beta'}^{(4*)}$, have the same symmetry but differ by a topological winding number of the order parameter $\mathbf{m}$. This winding number is 1 for the $P_{\beta'}^{(3*)}$ phase, while it is 0 for the $P_{\beta'}^{(4*)}$ phase. Thus there may or may not be a first-order transition between these structures with different winding number, but the same symmetry. This phenomenon can occur for small $C_{\parallel}'$ even in a model with $D = 0$ in Eq. (25).

## V. CHIRAL STRIPE PHASES AND LOW-TEMPERATURE THEORY

In the preceding sections, we have investigated Landau theory for the formation of $P_{\beta'}$ phases. This theory works best in the vicinity of the Lifshitz point where the tilt order parameter $\mathbf{m}$ is small. At low temperature, where the magnitude of $\mathbf{m}$ is essentially fixed, an alternative theory in which only the direction of $\mathbf{m}$ can vary is more appropriate. For achiral membranes, it can be shown that in this limit only three phases are possible. These are the $L_{\beta'}$, $P_{\beta'}^{(1)}$, and $P_{\beta'}^{(3)}$ phases described above. In chiral membranes, other modulated phases have been observed experimentally or predicted theoretically. In this section, we will investigate the formation of rippled structures from bend stripe patterns familiar in chiral free-standing liquid crystal films [26,28,29,31]. In particular, we will show that the curvature splay [Eq. (2)] and the Helfrich-Prost [Eq. (24)] contributions [30] to the free energy convert bend stripes into asymmetric ripples when the constraint that the membranes lie flat is relaxed. We will also show that the curvature splay coupling can lead to a period-doubling instability of the rippled structure.

There have been a number of models for the formation of bend stripe phases in smectic-$C^*$ films [26,28,29,31]. Here we will use the model employed by Selinger [31] in which membranes have both hexatic order with an order parameter $\psi_6 = |\psi_6|e^{6i\theta_6}$ and tilt order with order parameter $\psi_1 = m_x + im_y = |\psi_1|e^{i\theta_1}$. The low-temperature free energy density for a flat chiral film with this order is [31,32]

$$f_T = \frac{1}{2}K_6|\nabla\theta_6|^2 + \frac{1}{2}K_1|\nabla\theta_1|^2 + K_{16}\nabla\theta_1\cdot\nabla\theta_6 + V(\theta_1-\theta_6) - \lambda\mathbf{N}\cdot(\nabla\times\mathbf{m})\cos[6(\theta_1-\theta_6)], \quad (30)$$

where $\mathbf{N}$ is the unit normal to the film and $V(\theta) = V(\theta + (2\pi/6))$. The last term proportional to $\nabla\times\mathbf{m}$ is permitted in chiral but not in achiral films. A term linear in $\mathbf{N}\cdot(\nabla\times\mathbf{m})$ is also permitted, but in the present application it integrates to the sample boundary and can be ignored. In what follows, we will take $V(\theta) = V(1-\cos\theta)$. The change of variables

$$\theta_+ = \alpha\theta_6 + (1-\alpha)\theta_1,$$
$$\theta_- = \theta_6 - \theta_1, \quad (31)$$

permits decoupling of the variables $\theta_+$ and $\theta_-$ when $\lambda = 0$:

$$f_T = f_+ + f_- + f_{\rm ch}, \quad (32)$$

where

$$f_- = \frac{1}{2}K_-(\nabla\theta_-)^2 + V(1-\cos 6\theta_-), \quad (33)$$

$$f_+ = \frac{1}{2}K_+(\nabla\theta_+)^2, \tag{34}$$

$$f_{\rm ch} = -\lambda \mathbf{N}\cdot(\nabla\times\mathbf{m})\cos 6\theta_-, \tag{35}$$

where $K_+ = K_6 + K_1 + 2K_{16}$, $K_- = (K_1K_6 - K_{16}^2)/K_+$, and $\alpha = (K_6 + K_{16})/K_+$. If $K_6 \gg K_1, K_{16}$, then $K_+ \approx K_6$, $K_- \approx K_1 \ll K_6$, $\alpha \approx 1$, and $\theta_+ \approx \theta_6$. We will use this limit in what follows.

Before investigating height ripples, we will review briefly how $f_{\rm ch}$ leads to a modulated bend stripe phase. If $\theta_-$ is a constant, then $f_{\rm ch}$ integrates to the sample boundary and does not contribute extensively to the free energy. Interior boundaries can be introduced by domain walls (or solitons) in $\theta_-$. Thus stripes will be favored when the energy gain from $f_{\rm ch}$ at wall boundaries overcomes the energy cost of creating walls. We will, therefore, consider a linear array of walls of width $w$ separated by stripes of width $L$ depicted in Fig. 10. The energy of this structure can be estimated using a simple variational form for $\theta_1$:

$$\theta_1(x) = \begin{cases} -(\pi/6) + (\pi x/3L) & \text{if } 0 < x < L \\ (\pi/6) - [\pi(x-L)/3w] & \text{if } L < x < L+w, \end{cases} \tag{36}$$

as shown in Fig. 10. In the stripe region ($0 < x < L$), $\theta_6 = \theta_1$ and $\theta_- = 0$, whereas in the wall region ($L < x < L + w$), $\theta_6 = \pi/6$, and $\theta_- = (\pi/3w)(x - L)$. With these forms for $\theta_1$, $\theta_6$, and $\theta_-$, we can estimate the various

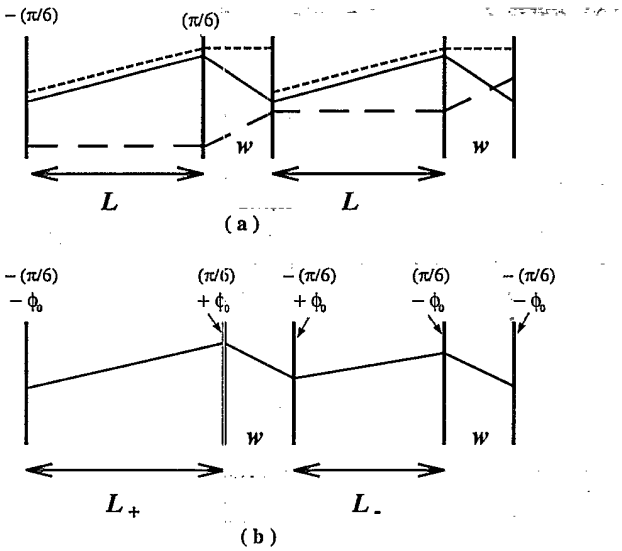


FIG. 10. (a) Schematic representation of stripes and walls in a bend stripe phase. The stripes are of width $L$, and the walls are of width $w$. The full line shows $\theta_1(x)$ as described by Eq. (36). The wide dashed line shows $\theta_-$, and the finely dashed line shows $\theta_6(x) \mathrm{mod} \pi/3$. At $x = 0$ and $x = L + w$, $\theta_1 = -\pi/6$, and at $x = L$, $\theta_1 = +\pi/6$. (b) Schematic representation of a unit cell of a period-doubled structure. There are now two stripe regions with respective lengths $L_+ = L(1+\rho)$ and $L_- = L(1-\rho)$. The full line shows $\theta_1(x)$. The values of $\theta_1$ at $x = 0$, $x = L_+$, $x = L_+ + w$, $x = L_+ + L_- + w$, and $x = L_+ + L_- + 2w$ are indicated.

contributions to the free energy per unit cell:

$$F_- = \int_0^{L+w} dx f_- = \frac{1}{2}K_-\frac{(\Delta\theta)^2}{w} + Vw, \tag{37}$$

$$F_+ = \int_0^{L+w} dx f_+ = \frac{1}{2}K_+\frac{(\Delta\theta)^2}{L}, \tag{38}$$

$$\begin{aligned} F_{\rm ch} &= \int_0^{L+w} dx f_{\rm ch} \\ &= -\lambda\int_0^L dx\frac{dm_y}{dx} - \lambda\int_L^{L+w} dx\frac{dm_y}{dx}\cos 6\theta_- \\ &= -\lambda[m_y(L) - m_y(0)] = -2\lambda\sin(\Delta\theta/2) = -\lambda, \end{aligned} \tag{39}$$

where $\Delta\theta = \theta(L) - \theta(0) = \pi/3$. Note that the contribution to $F_{\rm ch}$ coming from the wall region vanishes; the nonzero contribution to this function arises entirely from the boundary to the stripe region where $\cos 6\theta_- = 1$. The free energy per unit area is thus

$$f = \frac{1}{L+w}\left[\frac{1}{2}K_-\frac{(\Delta\theta)^2}{w} + Vw + \frac{1}{2}K_+\frac{(\Delta\theta)^2}{L} - \lambda\right]. \tag{40}$$

Minimizing this equation over $w$, we obtain the wall width $w = \Delta\theta(K_-/2V)^{1/2}$, and wall energy $\epsilon = \Delta\theta(2K_-V)^{1/2}$. Then

$$f = \frac{1}{L}\left[(\epsilon - \lambda) + \frac{1}{2}K_+\frac{(\Delta\theta)^2}{L}\right], \tag{41}$$

when $L \gg w$. Finally, minimizing this expression over $L$, we find $L^{-1} = 0$ for $\epsilon - \lambda > 0$ and $L^{-1} = (\Delta\theta)^{-2}K_+^{-1}|\epsilon - \lambda|$ for $\epsilon - \lambda < 0$. Thus there is a transition from a spatially uniform to a modulated structure when the chiral energy $\lambda$ exceeds the wall energy $\epsilon$.

If the constraint that the membrane be flat is removed, then the curvature splay energy $f_c$ [Eq. (2)] and the Helfrich-Prost energy [Eq. (24)], which in the present context can be written as

$$f_{\rm HP} = -\lambda_{\rm HP}\frac{d^2h}{dx^2}m_x m_y, \tag{42}$$

will immediately lead to height modulations once $\nabla\cdot\mathbf{m}$ and/or $m_x m_y$ are spatially modulated, as they are in the stripe phase just considered. Minimizing $f_c + f_{\rm HP}$ over $h$, we find

$$\frac{d^4h}{dx^4} = \frac{\gamma}{\kappa}\frac{d^3m_x}{dx^3} + \frac{\lambda_{\rm HP}}{\kappa}\frac{d^2}{dx^2}m_x m_y. \tag{43}$$

To lowest order in $\gamma/\kappa$ and $\lambda_{\rm HP}/\kappa$, we can determine $h(x)$ by integrating Eq. (43) with $\theta_1$ given by Eq. (36) subject to the boundary condition $h(0) = h(L+w)$. The result, depicted in Fig. 11 is

$$\begin{aligned} h(x) = \frac{\gamma}{\kappa}&\left[I_1(x) - \frac{x}{L+w}I_1(L+w)\right] \\ &+\frac{\lambda_{\rm HP}}{2\kappa}\left[J_2(x) - \frac{x}{L+w}J_2(L+w)\right], \end{aligned} \tag{44}$$

where

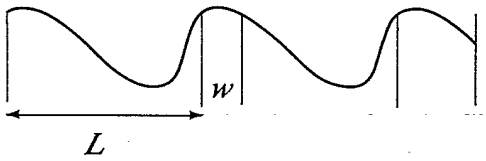


FIG. 11. The height profile $h(x)$ for a chiral bend stripe phase. The stripes are of width $L$ and the walls are of width $w$.

$$I_1(x) = \int_0^x dx \cos\theta_1(x),$$
$$J_2(x) = \int_0^x dx_1 \int_0^{x_1} dx_2 \sin[2\theta_1(x_2)]. \quad (45)$$

This height ripple has the same symmetry as the asymmetric ripples of Fig. 3(b) (i.e., the symmetry of the $P_{\beta'}^{(3*)}$ phase).

The splay bend term is in many ways similar to the chiral coupling, which is responsible for the formation of the bend stripe phase. If the curvature $d^2h/dx^2$ is constant, then $\nabla \cdot \mathbf{m}$ will integrate to the boundary of the sample and not contribute extensively to the energy. Artificial boundaries, analogous to the domain walls of the bend stripe phase, allowing $f_c$ to contribute extensively to the energy can be produced by a regular array of walls with constant curvature separated by regions of zero curvature. We will now show how this effect can lead to a period doubling of the bend stripe structure. For simplicity, we will consider only configurations in which the curvature $d^2h/dx^2 = R^{-1}$ is either a constant or zero and ignore modulations described by Eq. (44). Inclusion of the latter will not affect our general conclusions but would considerable complicate our algebra.

Consider a period-doubled array of stripes and walls, one unit cell of which is shown in Fig. 10. Here there are two striped regions with respective widths

$$L_\pm = L(1 \pm \rho) , \quad (46)$$

and two wall regions, whose width we will for simplicity take to be the same and equal to $w$. The curvature energy for a region $x_L < x < x_R$ with constant curvature is

$$F_c = \int_{x_L}^{x_R} dx f_c$$
$$= \frac{1}{2}(x_R - x_L)R^{-2} - \gamma R^{-2}[m_x(x_R) - m_x(x_L)]. \quad (47)$$

In the striped regions of Fig. 10, $m_x(x_R) = m_x(x_L)$, and a nonzero curvature is not favored. In the wall regions, on the other hand, $m_x(x_R) - m_x(x_L) = \cos[-(\pi/6) \pm \phi_0] - \cos[(\pi/6) \pm \phi_0] = \pm \sin\phi_0$. Thus, in a wall,

$$R^{-1} = \pm \frac{\gamma \sin\phi_0}{\kappa w} \quad (48)$$

and

$$F_c^{\pm} = \frac{1}{2}\frac{\gamma^2}{\kappa}\frac{\sin^2\theta_0}{w}. \quad (49)$$

The stripe and wall energies can now be calculated as before. $F_-$ [Eq. (37)] has contributions only from the wall and is identical for both walls. $F_+$ has the same form as Eq. (38) but with $L$ replaced by $L_+$ or $L_-$. $F_{\rm ch}$ in the $\pm$ stripe regions is $-2\lambda \sin[(\pi/6) \pm \phi_0]$. In addition, $F_{\rm ch}$ now has contributions from the two walls, which are equal and opposite in sign and therefore cancel. Thus the free energy per unit area is

$$f = \frac{1}{2L}\left[\left(K_- - \frac{\gamma^2}{\kappa}\sin^2\phi_0\right)\frac{1}{w} + 2Vw - 2\lambda\cos\phi_0 + \frac{1}{2}\frac{K_+}{L}\frac{(\Delta\theta + 2\phi_0)^2}{1+\rho} + \frac{1}{2}\frac{K_+}{L}\frac{(\Delta\theta - 2\phi_0)^2}{1-\rho}\right], \quad (50)$$

where we used $\sin[(\pi/6) + \phi_0] + \sin[(\pi/6) - \phi_0] = \cos\phi_0$. This equation can be expanded in a power series in $\phi_0$ and $\rho$. The resulting expression when minimized over $\rho$ yields

$$\rho = 6\phi_0/\pi, \quad (51)$$

and an effective free energy in terms of $\phi_0$,

$$f_{\rm eff} = f(\phi_0 = 0, \rho = 0) + \frac{1}{2L}\left[\left(\lambda - \frac{\gamma^2}{\kappa w}\right)\phi_0^2 + u\phi_0^4\right]. \quad (52)$$

The coefficient $u$ is a function of $\kappa$, $w$, $\lambda$, and $K_+$ and is positive. Thus, there will be a second-order transition to a period-doubled state with $\phi_0$ and $\rho$ nonzero for $\gamma^2/\kappa w > \lambda$.

## VI. RESULTS AND DISCUSSION

In the previous sections, we have presented a phenomenological model for modulated phases in both achiral and chiral membranes. For achiral membranes we expect that there can be more than one thermodynamically *distinct* ripple phase. These phases are expected to exhibit the *same ripple shape*—or, more precisely, the same symmetry with respect to membrane shape. These phases are distinguished by their *different* symmetry with respect to the tilt $\mathbf{m}$. For chiral membranes, these phases become distinguishable both in their shape and tilt $\mathbf{m}$. In particular, the $P_{\beta'}^{(3*)}$ phase is predicted to have the same symmetry as the "asymmetric" ripple structure observed both by x-ray diffraction and freeze-fracture images in numerous experiments.

The mean-field phase diagram for achiral membranes is shown in Fig. 9. This phase diagram is obtained within the variational approximation in Eqs. (6a) and (6b). The critical point with $C_\parallel' = 0$ at which order first develops is a Lifshitz point. The high-temperature disordered phase with $\mathbf{m} = \mathbf{0}$ is the $L_\alpha$ phase. The uniform phase with $\mathbf{m} \neq \mathbf{0}$ is the $L_{\beta'}$ phase. The modulated $P_{\beta'}^{(1)}$ and square lattice phases meet the $L_\alpha$ and $L_{\beta'}$ phases at the Lifshitz point. The "spiral" $P_{\beta'}^{(3)}$ phase is stable in a region below the Lifshitz point as shown in Fig. 9. The tran-

sition between it and the $P_{\beta'}^{(1)}$ phase is first order. At low temperature, the spiral $P_{\beta'}^{(3)}$ phase is further stabilized because the direction of the tilt $\mathbf{m}$ can vary, but the magnitude of the tilt becomes fixed. Due to the symmetry between splay and bend in the free energy in Eq. (1), the phase diagram of varying $C_\perp$ and $t$ is similar to Fig. 9 but with $\mathbf{m}$ rotated by $\pi/2$.

In addition to one-dimensional ripple phases, our model predicts the possible existence of a two-dimensional, square lattice modulated phase. Since only one-dimensional modulations have been observed in lipid-water mixtures, we have focused on these structures in this work. Stability considerations for two-dimensional modulated structures in lipid-water and related systems are more subtle than for one-dimensional ripples. In particular, we describe in Sec. III how positional order or hexatic order can destabilize two-dimensional modulated structures. We note, however, that our model is also applicable to thermotropic films, for which one or more square lattice modulated phases have been reported [33].

## ACKNOWLEDGMENTS

T.C.L. acknowledges support from the NSF under Grants No. DMR-91-20668 and No. DMR 91-22645. C.-M.C. and F.C.M. acknowledge partial support from the Donors of the Petroleum Research Fund, administered by the American Chemical Society, from the Exxon Education Fund, and from the NSF under Grant No. DMR-9257544. T.C.L. and F.C.M. are grateful for the hospitality of the Aspen Institute for Physics where a part of this work was carried out. The authors also wish to acknowledge helpful discussions with J. Selinger, J. Katsaras, and D. Mukamel.

[1] A. Tardieu, V. Luzzati, and F.C. Reman, J. Mol. Biol. **75**, 711 (1973).
[2] E.B. Sirota, G.S. Smith, C.R. Safinya, R.J. Plano, and N.A. Clark, Science **242**, 1406 (1988).
[3] M.J. Janiak, D.M. Small, and G.G. Shipley, Biochemistry **15**, 4575 (1976).
[4] E.J. Luna and H.M. McConnell, Biochim. Biophys. Acta **466**, 381 (1977).
[5] J.A.N. Zasadzinski, J. Schneir, J. Gurley, V. Elings, and P.K. Hansma, Science **239**, 1013 (1988).
[6] D.C. Wack and W.W. Webb, Phys. Rev. Lett. **61**, 1210 (1988).
[7] T.C. Lubensky and F.C. MacKintosh, Phys. Rev. Lett. **71**, 1565 (1993).
[8] J. Stamatoff, B. Feuer, J. Guggenheim, G. Tellez, and T. Yamane, Biophys. J. **38**, 217 (1982).
[9] M.P. Hentschel and F. Rustichelli, Phys. Rev. Lett. **66**, 903 (1991).
[10] J.T. Woodward and J.A.N. Zasadzinski (unpublished).
[11] R.B. Meyer and P.S. Pershan, Solid State Commun. **13**, 989 (1973); R.B. Meyer, L. Liebert, L. Strzelecki, and P. Keller, J. Phys. (Paris) Lett. **36**, L69 (1975); J. Maclennan, Europhys. Lett. **13**, 435 (1990).
[12] J.A.N. Zasadzinski, Biochim. Biophys. Acta **946**, 235 (1988).
[13] P. Meier, A. Blume, E. Ohmes, F.A. Neugebauer, and G. Kothe, Biochemistry **21**, 526 (1982).
[14] M.S. Falkovitz, M. Seul, H.L. Frisch, and H.M. McConnell, Proc. Nat. Acad. Sci. U.S.A. **79**, 3918 (1982).
[15] M. Marder, H.L. Frisch, J.S. Langer, and H.M. McConnell, Proc. Nat. Acad. Sci. U.S.A. **81**, 6559 (1984).
[16] R.E. Goldstein and S. Leibler, Phys. Rev. Lett. **61**, 2213 (1988).
[17] S. Doniach, J. Chem. Phys. **70**, 4587 (1979).
[18] J.M. Carlson and J.P. Sethna, Phys. Rev. A **36**, 3359 (1987).
[19] M. Tinkham, *Group Theory and Quantum Mechanics* (McGraw-Hill, New York, 1964).
[20] The symmetry groups are defined as follows. $S^{(a)} = \{1, \sigma_a\}$, where $\sigma_a$ is the reflection in the plane perpendicular to the $a$ axis; $C_n^{(a)}$ are the cyclic point groups that correspond to $n$-fold rotational symmetry about the $a$ axis; $C_{nv}^{(a)}$ have $n$ reflection planes containing the principal $n$-fold axis $a$; $C_{nh}^{(a)} = C_n^{(a)} \times S^{(a)}$; $D_n^{(a)}$ have $n$ two-fold rotation axes perpendicular to the principal $n$-fold axis $a$; $D_{nh}^{(a)} = D_n^{(a)} \times S^{(a)}$. We have suppressed the principal rotation axis wherever the $z$ axis is implied.
[21] Recent experiments carried out on isolated membranes have shown these ripple structures, as well [10]. Thus it appears that interactions between layers are not required for the formation of the ripple phase.
[22] R.M. Hornreich, M. Luban, and S. Shtrickman, Phys. Rev. Lett. **35**, 1678 (1975).
[23] If the membrane were under tension, there would be a term proportional to $(\nabla h)^2$ in $f_c$. A membrane in an equilibrium lamellar stack is effectively under zero tension, and Eq. (2) applies.
[24] F.C. MacKintosh and T.C. Lubensky, Phys. Rev. Lett. **67**, 1169 (1991).
[25] J.V. Selinger, Z.-G. Wang, R.F. Bruinsma, and C.M. Knobler, Phys. Rev. Lett. **70**, 1139 (1993).
[26] S.A. Langer and J.P. Sethna, Phys. Rev. A **34**, 5035 (1986).
[27] D. Blankschtein, E. Domany, and R.M. Hornreich, Phys. Rev. Lett. **49**, 1716 (1982); J. Felix, D. Mukamel, and R.M. Hornreich, *ibid.* **57**, 2180 (1986); A.E. Jacobs, G. Goldner, and D. Mukamel, Phys. Rev. A **45**, 5783 (1992).
[28] G.A. Hinshaw, R.G. Petschek, and R.A. Pelcovits, Phys. Rev. Lett. **60**, 1864 (1988).
[29] G.A. Hinshaw and R.G. Petschek, Phys. Rev. A **39**, 5914 (1989).
[30] W. Helfrich and J. Prost, Phys. Rev. A **38**, 3065 (1988).
[31] J.V. Selinger, in *Complex Fluids*, edited by E.B. Sirota, D. Weitz, T. Witten, and J. Israelachvili, MRS Symposia Proceedings No. 248 (Materials Research Society, Pittsburgh, 1992), p. 29.
[32] J.V. Selinger and D.R. Nelson, Phys. Rev. A **39**, 3135 (1989).
[33] E.B. Sirota, P.S. Pershan, and M. Deutsch, Phys. Rev. A **36**, 2902 (1987).